The tumor suppressor protein DLC1 maintains protein kinase D activity and Golgi secretory function

Antje Jensch, Yannick Frey, Katharina Bitschar, Patrick Weber, Simone Schmid, Angelika Hausser, Monilola A. Olayioye, Nicole E. Radde

July 24, 2018

Supporting Information

Contents

Table S1: Experimental data, normalized to the highest signal value

Experiment 1: Input PDBu, control (Fig. **S1**)								
time			pDLC1				pPKD	
0 min			0.05	0.18			0.00	0.08
5 min			0.60	0.24			0.39	0.47
20 min			0.72	0.29			0.56	0.73
60 min			1	1			1	1
Experiment 2: Input PDBu, kb-NB (Fig. **S1**)								
time			pDLC1				pPKD	
0 min			-	-			0.02	0.04
5 min			0.14	0.08			0.09	0.18
20 min			0.17	0.24			0.10	0.27
60 min			0.42	0.28			0.15	0.43
Experiment 3: Input nocodazole, control (Fig. 2A)								
time			pDLC1				pPKD	
0 min	0.32	0.66	0.57	0.36	0.28	1.60	0.52	0.46
10 min	0.72	0.74	0.96	0.85	0.80	1.39	0.89	0.68
30 min	1	1	1	1	1	1	1	1
Experiment 4: Input nocodazole, kb-NB (Fig. 2A)								
time			pDLC1				pPKD	
10 min	0.26	0.50	0.54	0.79	0.57	0.92	0.69	0.75
30 min	0.96	0.72	0.78	0.83	0.98	0.97	0.80	1.06
Experiment 5: Input nocodazole, Gö-6976 (Fig. 2A)								
time			pDLC1				pPKD	
10 min	0.11	0.44	0.46	0.49	0.33	0.20	0.71	0.59
30 min	0.09	0.16	0.54	0.47	0.64	0.65	0.77	0.57
Experiment 6: pPKD and pDLC1, control (Fig. 1B)								
			pDLC1				pPKD	
	0.14	0.86	0.80		0.53	0.31	0.41	
Experiment 7: pPKD and pDLC1, Rho ca (Fig. 1B)								
			pDLC1				pPKD	
	1	1	1		1	1	1	

1 Positive feedback model (model 1): Data pre-processing

1.1 Additional experimental data

Fig. **S1** shows PKD and DLC1 phosphorylation time courses after stimulation with the phorbol ester PDBu, in the absence or presence of the PKD inhibitor kb-NB.

1.2 Normalization of experimental data

Western blot data are usually normalized in a multi-step procedure, including background corrections and normalization to a loading control to diminish spurious signals resulting from loading differences. Further normalization is required to enable a comparison across different replicates. For this purpose, normalization to a control experiment is a commonly applied standard procedure, which we also use in this study. Normalization is an important data pre-processing step, which also affects the statistical properties of the normalized data [8, 10] and therefore has an impact on state estimation and hypothesis testing. In accordance with [3], we re-normalized experimental data to the highest signal value to avoid normalization to values with low signal-to-noise ratios. Respective data is shown in Table **S1**.

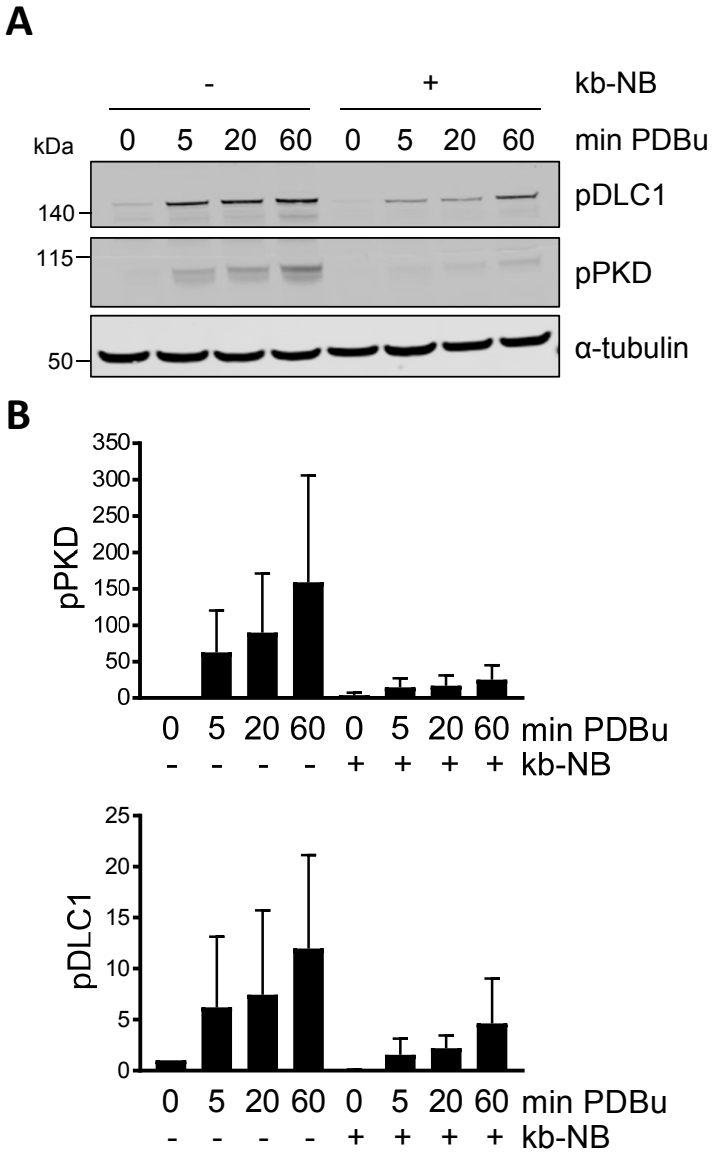

Fig S1: (A) Expression of GFP-DLC1 in Flp-In GFP-DLC1 was induced with doxycycline. The next day, cells were treated with the PKD inhibitor kb NB 142-70 for 2 h, followed by PDBu treatment for the times indicated. Cells lysates were analyzed by immunoblotting. (B) Band intensities from four independent experiments were quantified and normalized to the loading control and control sample (mean ± SEM).

1.3 Significance test for the effect of inhibitors kb-NB and Gö-6976

Significance of the effect of the inhibitors kb-NB and Gö-6076 was investigated by setting up a parametrized dynamic model and using an F-test. For this, we defined and compared two nested parametrized model variants for each inhibitor. In the null hypothesis H_0, the inhibitor does not act significantly and hence the data can be described with a single parametrized hyperbolic curve,

$$H_0: \quad \varphi(t) = \varphi_0 + 1 - \exp(-\lambda t), \tag{1}$$

with parameters φ_0 and λ. The alternative hypothesis H_1 assumes a significant influence of the inhibitor under investigation on the pPKD and pDLC1 time courses. Therefore, two curves $\varphi^c(t)$ and $\varphi^i(t)$ were defined for the control and inhibition experiment, respectively:

$$H_1: \quad \varphi^c(t) = \varphi_0^c + 1 - \exp(-\lambda^c t) \tag{2a}$$

$$\varphi^i(t) = \varphi_0^i + b^i(1 - \exp(-\lambda^i t)), \tag{2b}$$

with parameters φ_0^c, λ^c, φ_0^i, b^i and λ^i, where superscripts c and i symbolize the control and the inhibition experiments, respectively.

For model calibration we chose the method of least squares with normalized data taken from Table **S1**. The normalization point at $t = 30$ min was taken into account by a constraint on φ_0,

$$\varphi(30\,\text{min}) = 1 = \varphi_0 + 1 - \exp(-\lambda \cdot 30\,\text{min}), \tag{3}$$

leading to $\varphi_0 = \exp(-\lambda \cdot 30\,\text{min})$. Analogously, we set $\varphi_0^c = \exp(-\lambda^c \cdot 30\,\text{min})$ for H_1. We define $y_{j,l}^c(t_k)$ and $y_{j,l}^i(t_k)$ as measurement outputs for the control and inhibition experiment, respectively. Thus, the residual sum of squares for H_0 was specified as

$$RSS_{1,j} = \sum_{t_k} \sum_{l=1}^{4} \left[(y_{j,l}^c(t_k) - \varphi(t_k))^2 + (y_j^i(t_k) - \varphi(t_k))^2 \right] \tag{4}$$

and respectively for H_1

$$RSS_{2,j} = \sum_{t_k} \sum_{l=1}^{4} \left[(y_{j,l}^c(t_k) - \varphi^c(t_k))^2 + (y_{j,l}^i(t_k) - \varphi^i(t_k))^2 \right], \tag{5}$$

where $j \in \{\text{pPKD, pDLC1}\}$, $k = 1, \ldots, 3$ and $l = 1, \ldots, 4$ denote outputs, the time points with $t_k \in \{0, 10, 30\}$min and the number of replicates per experimental condition. For parameter estimation the residual sum of squares was minimized separately for both measurement outputs using the `fmincon` algorithm in `Matlab 2016b` (64 bit). All optimizer options were set to default with parameter boundaries from 0 to 5 on a linear scale. A multistart optimization using 1000 starting points was performed for all model variants and measurement outputs.

The F-value for the F-test was calculated via

$$F = \frac{\dfrac{RSS_1 - RSS_2}{p_2 - p_1}}{\dfrac{RSS_2}{n_{\text{data}} - p_2}}, \tag{6}$$

with

$$RSS_1 = RSS_{1,\text{pPKD}} + RSS_{1,\text{pDLC1}} \tag{7a}$$

$$RSS_2 = RSS_{2,\text{pPKD}} + RSS_{2,\text{pDLC1}}. \tag{7b}$$

The constants $p_1 = 2$ and $p_2 = 8$ denote the numbers of parameters for H_0 and H_1, respectively. The total number of data points including pPKD and pDLC1 time course data was $n_{\text{data}} = 32$. In order to test H_0, we consider the tails of the $\mathcal{F}$-distribution with $(p_2 - p_1, n_{\text{data}} - p_2)$ degrees of freedom. An $\alpha = 5\%$ level of significance corresponds to a critical value $F_\alpha = 2.51$, and H_0 is rejected if the observed F value exceeds F_α. Results of this testing procedure are shown in Fig. 2B of the main manuscript.

1.4 Selection of an error model

For model calibration we exploit maximum-likelihood estimation, which requires the choice of an appropriate error model for observed outputs. Additive normally distributed error models or multiplicative log-normal error models are most frequently used for this purpose. In Kreutz et al. [8] it was argued that the main source of biological variability and experimental noise is multiplicative and log-normally distributed, which suggests a log-transformation of the data to obtain approximately normally distributed data. The mixed error model from which additive and multiplicative effects are deduced in [8] is, however, not applicable in our setting due to low numbers of replicates per condition. Here we decided to select an error model as a data-driven pre-processing step on the normalized data. Such an a priori analysis is computationally more attractive than integrating the selection of an error model directly into model calibration and allows for a much more comprehensive comparison of different error models. We used additive normal and multiplicative log-normal error models, in combination with maximum-likelihood estimators for the means and the variances. Since the maximum-likelihood variance estimator is biased, we additionally included also unbiased variance estimators. Moreover, we compared independent standard deviation estimation for each condition and each time point with the estimation of partly pooled standard deviations. The first pooling version averages the standard deviation of each experimental condition separately for each output, resulting in 12 standard deviation parameters. For the second pooling the standard deviations were further averaged per Western blot according to Fig. 1A, 2A and **S1**A. We compared all model variants by using different information criteria. Results are shown in Table **S2**. Shown are the likelihood values $\mathcal{L}$, the Akaike information criterion (AIC), the corrected Akaike information criterion (AIC_c), the Bayesian information criterion (BIC) and Akaike weights, i.e.

$$\Delta_i = \mathrm{AIC}_{c_i} - \min(\mathrm{AIC}_c)$$
$$\mathrm{AW}_i = \frac{\exp(-\Delta_i/2)}{\sum_{r=1}^{R}\exp(-\Delta_r/2)}.$$

For each case, the three superior ones are color marked. The AIC agrees with the likelihood values in the choice of the best model. Both select the most complex model. This selection is, however, different from that of AIC_c, BIC and AW, all of which also agree in the choice of the best error model. Overall, these results reflect that the later penalize complexity more than the AIC. It should be noted here that both AIC and BIC are approximations that assume a large sample size compared to the number of parameters [1, 9], which is not given here. Thus we judge AIC_c, which corrects for finite sample sizes [2], and Akaike weights the more suitable criteria here, which also completely agree in their ranking. Hence we decided to select the most plausible error model according to these two criteria. According to the evidence Table in [7], AIC_c records positive evidence between the best and the second best model. Based on these results, we decided to use an additive normal error model and six standard deviation for the following modeling study. The six standard deviation pools are represented by six parameters σ_j^i, $i = 1, 2, 3$, $j \in \{\mathrm{pPKD}, \mathrm{pDLC1}\}$ depicting the standard deviation for each experiment and output pooled as described above. Table **S3** shows the composition of experiments that were used for pooling.

2 Model 1: Modeling and model calibration

In the following we provide details on the positive feedback modeling approach and calibration to experimental data.

2.1 Modeling approach and normalization

According to Fig. 1E, we built up a simplified two state variable model,

$$\dot{\mathrm{pPKD}} = k(\mathrm{DLC1}, \theta)\mathrm{PKD} - \theta_1 \mathrm{pPKD} \tag{8a}$$
$$\dot{\mathrm{pDLC1}} = \theta_2 \mathrm{pPKD} \cdot \mathrm{DLC1} - \theta_3 \mathrm{pDLC1}, \tag{8b}$$

with model parameters θ. For simplicity and because the ratio of substrate and kinase molecules are unknown we used mass action kinetics wherever applicable. The PKD phosphorylation rate $k(\mathrm{DLC1}, \theta)$

Table S2: Error model selection procedure based on information criteria. In total $N = 80$ measurements were used. Standard deviations were either estimated individually for each condition and time point (σ_i), or by pooling over time series and outputs ($\bar{\sigma}_{12}$) or over experiments and outputs ($\bar{\sigma}_6$). The three superior models are marked in green (top), orange (second top) and yellow (third top).

Error model	# parameters	$\mathcal{L}$	AIC	AIC_c	BIC	AW
$\mathcal{N}$, unbiased, σ_i	54	1.0e25	-7.19	230.41	121.44	3.5e-41
$\mathcal{N}$, unbiased, $\bar{\sigma}_{12}$	39	1.4e20	-14.73	63.27	78.17	6.9e-05
$\mathcal{N}$, unbiased, $\bar{\sigma}_6$	33	1.7e15	-4.14	44.64	74.46	0.7662
$\mathcal{N}$, biased, σ_i	54	3.9e26	-14.45	223.15	114.18	1.3e-39
$\mathcal{N}$, biased, $\bar{\sigma}_{12}$	39	4.9e20	-17.30	60.70	75.60	0.0002
$\mathcal{N}$, biased, $\bar{\sigma}_6$	33	5.2e14	-1.75	47.03	76.85	0.2317
log $\mathcal{N}$, unbiased, σ_i	54	7.6e25	-11.18	226.42	117.45	2.6e-40
log $\mathcal{N}$, unbiased, $\bar{\sigma}_{12}$	39	1.9e18	-6.21	71.79	86.69	9.7e-07
log $\mathcal{N}$, unbiased, $\bar{\sigma}_6$	33	3.6e12	8.19	56.97	86.79	0.0016
log $\mathcal{N}$, biased, σ_i	54	2.7e27	-18.44	219.16	110.19	9.7e-39
log $\mathcal{N}$, biased, $\bar{\sigma}_{12}$	39	2.1e18	-6.41	71.59	86.49	1.1e-06
log $\mathcal{N}$, biased, $\bar{\sigma}_6$	33	1.9e11	14.08	62.86	92.69	8.4e-05

Table S3: Experiments and states used for calculation of the six standard deviation pools depending on the experimental conditions given in Table **S1**.

variance parameter	pooled experiments (state variable)
σ^1_{PKD}	1,2 (pPKD)
σ^2_{PKD}	3,4,5 (pPKD)
σ^3_{PKD}	6 (pPKD)
σ^1_{DLC1}	1,2 (pDLC1)
σ^2_{DLC1}	3,4,5 (pDLC1)
σ^3_{DLC1}	6 (pDLC1)

Table S4: PKD phosphorylation rate $k(\mathrm{DLC1}, \theta)$ depending on the experimental setup and on DLC1

Treatment (u, α)	$k(\mathrm{DLC1}, \theta)$	Remark
–	$\begin{cases} \theta_0(1-\theta_6\mathrm{DLC1}) & \theta_6\mathrm{DLC1} \in [0,1] \\ 0 & \text{otherwise} \end{cases}$	unphosphorylated DLC1 decreases the basal PKD phosphorylation rate
PDBu	$k + \theta_4$	PDBu triggers PKD phosphorylation
Noc	$k + \theta_5$	nocodazole triggers PKD phosphorylation
kb-NB	$\begin{cases} k(1-\theta_8) & \theta_8 \in [0,1] \\ 0 & \text{otherwise} \end{cases}$	kb-NB decreases the overall PKD phosphorylation rate
Gö-6976	$\begin{cases} k(1-\theta_7) & \theta_7 \in [0,1] \\ 0 & \text{otherwise} \end{cases}$	Gö-6976 acts similar to kb-NB
Rho ca	$k + \theta_9$	constitutively active Rho increases PKD phosphorylation

depends on DLC1 via Rho and on the experimental treatment of the cell culture and is specified in Table **S4** for the different treatments used for model calibration.

We eliminated PKD and DLC1 by assuming mass conservation of respective total amounts,

$$\mathrm{PKD}_{\mathrm{tot}} = \mathrm{PKD} + \mathrm{pPKD} \tag{9a}$$
$$\mathrm{DLC1}_{\mathrm{tot}} = \mathrm{DLC1} + \mathrm{pDLC1}. \tag{9b}$$

Normalization of both state variables to total concentrations,

$$x_1 = \frac{\mathrm{pDLC1}}{\mathrm{DLC1}_{\mathrm{tot}}} \tag{10a}$$
$$x_2 = \frac{\mathrm{pPKD}}{\mathrm{PKD}_{\mathrm{tot}}} \tag{10b}$$

leads to

$$\dot{x}_1 = (\theta_0(1-\tilde{\theta}_6(1-x_2)) + \theta_4 u_1 + \theta_5 u_2 + \alpha_3\theta_9)(1-\alpha_1\theta_7 - \alpha_2\theta_8)(1-x_1) - \theta_1 x_1 \tag{11a}$$
$$\dot{x}_2 = \tilde{\theta}_2(1-x_2)x_1 - \theta_3 x_2 \tag{11b}$$

where $\tilde{\theta}_6 = \theta_6\mathrm{DLC1}_{\mathrm{tot}}$, $\tilde{\theta}_2 = \theta_2\mathrm{DLC1}_{\mathrm{tot}}$ and u_i, α_i are Boolean variables that are used to indicate the treatment. For the sake of simplicity the parameters $\tilde{\theta}_6$ and $\tilde{\theta}_2$ will be called θ_6 and θ_2 in the following. Together with the standard deviations of the error model, the vector of unknown parameters is given by

$$\boldsymbol{\theta} = (\theta_0, \theta_1, \theta_2, \theta_3, \theta_4, \theta_5, \theta_6, \theta_7, \theta_8, \theta_9, \sigma^1_{\mathrm{PKD}}, \sigma^2_{\mathrm{PKD}}, \sigma^3_{\mathrm{PKD}}, \sigma^1_{\mathrm{DLC1}}, \sigma^2_{\mathrm{DLC1}}, \sigma^3_{\mathrm{DLC1}}) \in \mathbb{R}^{16}_+.$$

2.2 Likelihood function

For model calibration we used maximum-likelihood estimation with the previously chosen error model. We also included the pooled standard deviations as optimization parameters in order to be more flexible with data points that cannot properly be fitted. We use $y_{ijl}(t_k)$ to denote measurement outputs. The indices $i = 1, \ldots, 7$, $j = 1, 2$, $k = 1, \ldots, 6$ and $l = 1, \ldots, 4$ denote different experimental conditions, enumeration of the outputs, the time points with $t_k \in \{0, 5, 10, 20, 30, 60\}$min and the number of replicates per experimental condition, respectively. According to the error model, we assume

$$Y_{ij}(t_k) \sim \mathcal{N}(z_{ij}(\boldsymbol{\theta}, t_k), \sigma^2_{ij}), \tag{12}$$

where z_{ij} denotes the normalized output according to Table **S1**,

$$z_{ij}(\boldsymbol{\theta},\, t_k) = \frac{x_{ij}(\boldsymbol{\theta},\, t_k)}{x_{\mathrm{ctrl},j}(\boldsymbol{\theta},\, t_{\mathrm{ctrl}})}, \tag{13}$$

where $x_{\mathrm{ctrl},\,j}$ is the value of the simulated substrate j under the conditions of the experimental data used for normalizing y_{ij} and t_{ctrl} is the normalization time point.

The likelihood function then reads

$$\mathcal{L}(\boldsymbol{\theta}) = p(y|\boldsymbol{\theta}) = \prod_{i=1}^{7}\prod_{j=1}^{2}\prod_{t_k}\prod_{l=1}^{4} \frac{1}{\sigma_{ij}\sqrt{2\pi}} \exp\left[-\frac{1}{2}\left(\frac{y_{ijl}(t_k) - z_{ij}(\boldsymbol{\theta}, t_k)}{\sigma_{ij}}\right)^2\right]. \tag{14}$$

We used the negative log-likelihood function for optimization,

$$\max_{\boldsymbol{\theta}\in\Theta} \mathcal{L}(\boldsymbol{\theta}) = \min_{\boldsymbol{\theta}\in\Theta} -\log \mathcal{L}(\boldsymbol{\theta}) = J_{\mathrm{opt}}, \tag{15}$$

where Θ is the set of acceptable parameters and J_{opt} is called the objective function value.

2.3 Optimization details

In order to evaluate the likelihood function (14), all simulations of the model (11) were performed via `Matlab 2016b` (64 bit). For model handling we used the `SBTOOLBOX2` and `SBPD` toolboxes, which make use of the CVODE solver from `SUNDIALS` for integration. Integrator options were set to `options.abstol = 1e-10` and `options.reltol = 1e-10`.

The optimization problem (15) was solved with the Pattern Search algorithm, which gave most reliable results in several tests for our setting. Pattern Search was introduced by [6] and uses a mesh in the parameter space in order to move step-wise to the minimum of the objective function. During a parameter poll a decrease in the objective function value is called a success and leads to an increase of the mesh size, whereas in case that the objective function value cannot be decreased the mesh size is reduced.

For implementation in `Matlab` we used the internal algorithm `patternsearch` with the following options:

- `OptionsPatternsearch.Cache = 'off'`,
- `OptionsPatternsearch.CompletePoll = 'off'`,
- `OptionsPatternsearch.MeshAccelerator = 'on'`,
- `OptionsPatternsearch.ScaleMesh = 'on'`,
- `OptionsPatternsearch.MaxFunEvals = 9000p`,
- `OptionsPatternsearch.MaxIter = 300p`,

where $p = 16$ is the number of unknown parameters.

As further options we set boundaries for these parameters. We used a logarithmic scale for the reaction rate parameters $\theta_0, \ldots, \theta_9$, which allows to cover many orders of magnitude. Our boundaries comprise four orders of magnitude and were adjusted through several optimization runs, such that the optima that were found do not lie on one of the boundaries. Boundaries for the parameters θ_7 and θ_8, the efficiencies of the two PKD inhibitors, were set to [0, 1] according to (11). For the standard deviations σ_j^i we used the empirical estimates σ_{emp} to set reasonable boundaries, which were finally set to $\sigma_j^i \in \left[\frac{2}{3}\sigma_{\mathrm{emp}},\ \frac{3}{2}\sigma_{\mathrm{emp}}\right]$.

Optimization was performed with 1000 latin hypercube samples as starting values. The initial conditions $x_1(0)$ and $x_2(0)$ were under steady state assumption calculated according to the conditions specified for each experiment. Fig. **S2** shows the resulting objective function values for 951 converged parameter sets[1], 929 of which form a nice plateau.

Figs. **S3** and **S4** show parameter scatterplots. The parameters $\theta_2, \theta_3, \theta_4, \theta_5, \theta_7$ and θ_8 are clearly identifiable from the experiments. It is also plausible that $\theta_5 > \theta_4$, since kb-NB is able to abolish the signal almost completely in case of stimulation with PDBu, while PKD is still considerably activated in case of stimulation with nocodazole. Similarly, θ_7 is close to the maximal value 1 and larger than the influence

[1] ensuring that the magnitude of the mesh size is less than the specified tolerance and constraint violation is less than those specified in options.ConstraintTolerance.

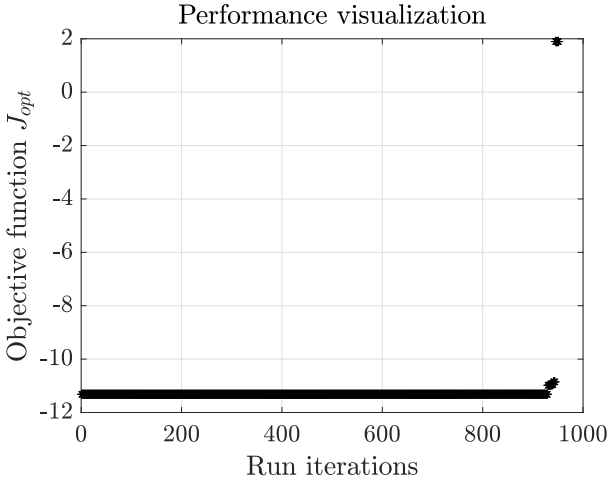

Fig S2: Sorted objective function values of converged parameter sets for model 1.

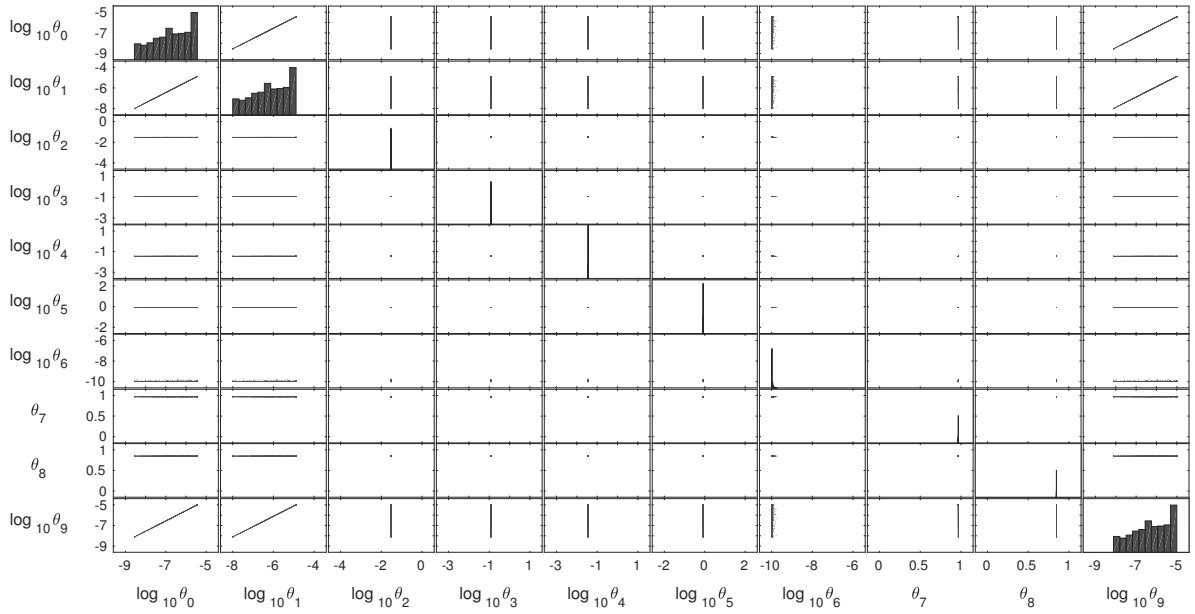

Fig S3: Scatterplot matrix for 929 parameter sets extracted from Figure **S2**.

of the inhibitor kb-NB, which also reflects experimental observations. The basal PKD phosphorylation and dephosphorylation rates θ_0 and θ_1, respectively, have a much larger uncertainty. This is also true for the parameter θ_9, which characterizes the effect of RhoA on PKD that also showed a high variance in the experiments. Surprisingly at first glance, these three parameters are almost perfectly correlated. Having a closer look at the parameters, this can easily be explained in the following way: The optimizer assigns quite small values to the parameter θ_6, which is a measure for the influence of DLC1 on PKD. Given this, PKD dynamics is hardly affected by DLC1. In this case, the strong correlations directly follow from a steady state analysis of decoupled PKD. The correlation between θ_0 and θ_1 follows from the steady state conditions in the control case, while the correlation of θ_9 with both parameters results from the observed steady state ratio conditions in the Rho ca experiments.

We used the 929 parameter sets from the plateau in Fig. **S2** to evaluate the model fit and to have an estimate of the resulting uncertainty due to non-identifiable parameters. In addition to the dynamic response of the system to nocodazole treatment with and without PKD inhibitors, which are shown in Fig. 2C in the main manuscript, Fig. **S5** shows the model fit after treatment with PDBu with and without inhibitor and steady state fold changes in PKD and DLC1 phosphorylation in the Rho ca experiments.

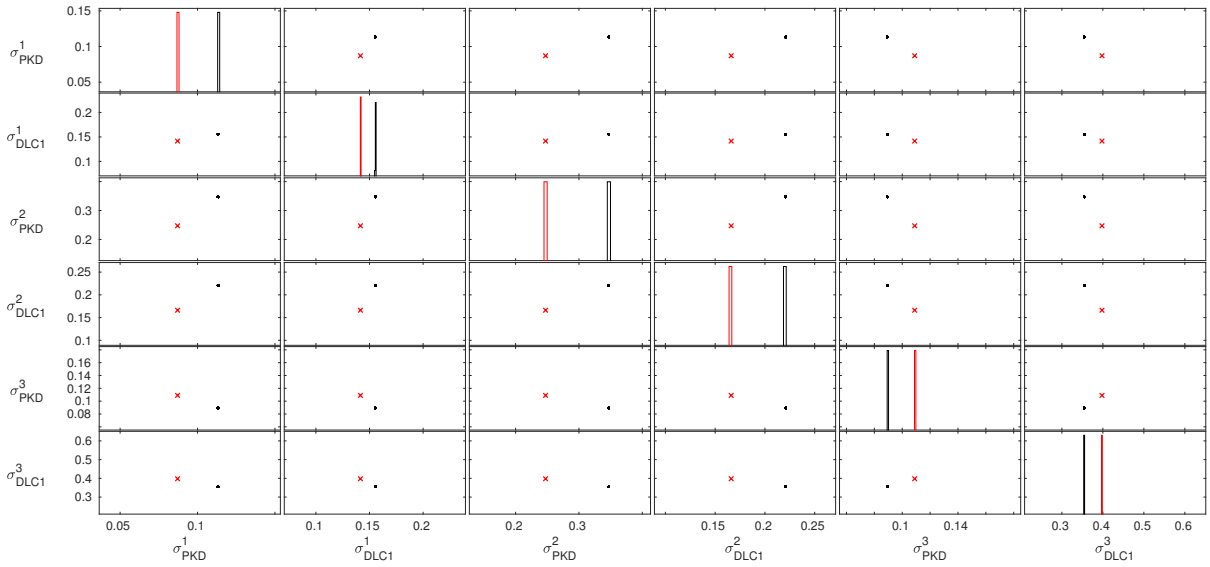

Fig S4: Scatterplot matrix of 929 standard deviations σ (black) in comparison with unbiased empirical estimates (red).

Overall, the response of the system is very well described. Experimental data and model trajectories agree well for pPKD and pDLC1 in the control case and in case cells were treated with the inhibitor kb-NB prior to PDBu treatment. Also the fold changes in pPKD and pDLC1 induced by constitutively active Rho are well captured by our model, though the variance in the data is quite large here, especially for pDLC1.

2.4 Model validation via bootstrapping

Plausibility of the model was tested with a parametric bootstrapping approach (see e.g. [4]), in which we generated many datasets from the inferred stochastic model, which were subsequently used to estimate a distribution of likelihood function values J (Fig. 2D). For this purpose, we resampled D_i, $i = 1, \ldots, 10000$ datasets that mimic experimental data used in the study (i.e. same number of replicates, same conditions etc.). Then we calculated $p(D_i|\hat{\theta})$ with σ_{ij} from $\hat{\theta}$ and used these values to estimate a probability density $p(J_{\text{opt}}) = p(D_i|\hat{\theta})$ via kernel density estimation, which was compared to $p(y|\hat{\theta})$, the likelihood value for the real experimental data.

2.5 Profile likelihood analysis

The profile likelihood shown in Fig. 3B was obtained by setting the feedback parameter θ_6 to the indicated value and re-optimizing all other parameters. For computational efficiency, we did not initialize all parameters from scratch in each of these optimization runs, but used the results from the previous run as a starting point for the next run.

3 Negative feedback model (model 2): Data pre-processing

3.1 Normalization of experimental data

For model calibration we used the normalization from Table **S1**. Additional experiments were normalized analogously, which is indicated in Table **S5**.

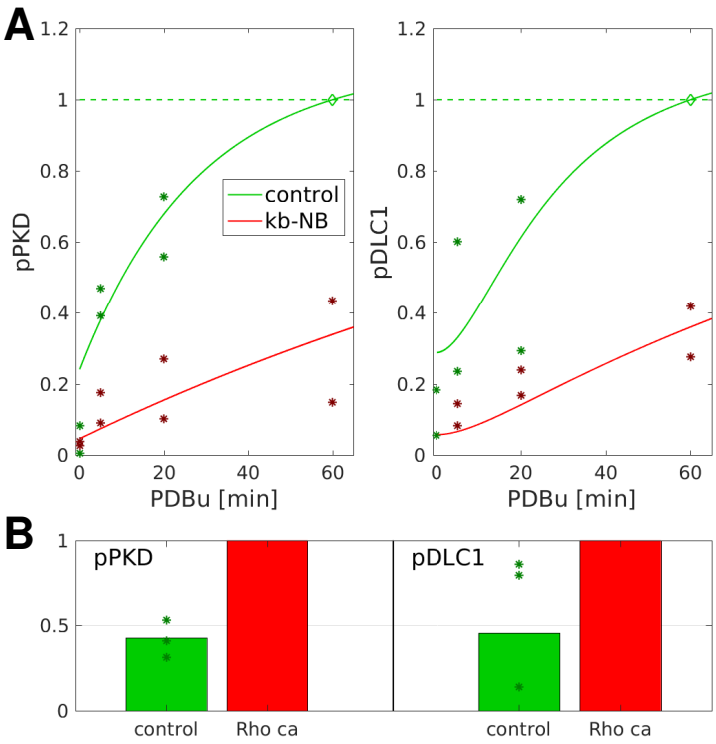

Fig S5: Fit for model 1. (A) Dots indicate re-normalized experimental data from Fig. S1, with normalization points indicated by diamonds, together with 929 estimated model trajectories that lie all on top of each other.

Table S5: Experimental data, normalized to the highest signal value

Experiment 8: -Dox (Fig. 4A)			
			pPKD
	0.38	1.08	0.89
Experiment 9: +Dox (Fig. 4A)			
			pPKD
	1	1	1
Experiment 10: Input nocodazole, siNT (Fig. 4B)			
time			pPKD
0 min	0.28	0.46	0.50
10 min	0.76	0.54	0.55
30 min	1	1	1
Experiment 11: Input nocodazole, siDLC1 (Fig. 4B)			
time			pPKD
0 min	0.09	0.13	0.17
10 min	0.45	0.37	0.54
30 min	0.72	0.53	0.82
Experiment 12: siNT, -H1152 (Fig. 4D)			
			pPKD
	1	1	1
Experiment 13: siDLC1, -H1152 (Fig. 4D)			
			pPKD
	0.26	0.53	0.37
Experiment 14: siDLC1, +H1152 (Fig. 4D)			
			pPKD
	0.76	0.71	0.45

Table S6: Error model selection procedure based on information criteria. In total $N = 104$ measurements were used. Standard deviations were either estimated individually for each condition (σ_i), or by pooling over time series and outputs ($\bar{\sigma}_{17}$) or over experiments and outputs ($\bar{\sigma}_9$). Color encoding was chosen equivalent to Table **S2**.

Error model	# parameters	$\mathcal{L}$	AIC	AIC$_c$	BIC	AW
$\mathcal{N}$, unbiased, σ_i	70	3.7e33	-14.61	286.60	170.49	2.2e-52
$\mathcal{N}$, unbiased, $\bar{\sigma}_{17}$	52	7.7e27	-24.42	83.65	113.08	2.6e-08
$\mathcal{N}$, unbiased, $\bar{\sigma}_9$	44	8.3e22	-17.56	49.56	98.79	0.6560
$\mathcal{N}$, biased, σ_i	70	3.4e35	-23.61	277.61	161.50	2.0e-50
$\mathcal{N}$, biased, $\bar{\sigma}_{17}$	52	4.7e28	-28.05	80.03	109.46	1.6e-07
$\mathcal{N}$, biased, $\bar{\sigma}_9$	44	4.3e22	-16.25	50.87	100.10	0.3407
log $\mathcal{N}$, unbiased, σ_i	70	1.6e34	-17.56	283.65	167.55	9.6e-52
log $\mathcal{N}$, unbiased, $\bar{\sigma}_{17}$	52	2.1e26	-17.26	90.82	120.25	7.2e-10
log $\mathcal{N}$, unbiased, $\bar{\sigma}_9$	44	3.7e20	-6.72	60.40	109.63	0.0029
log $\mathcal{N}$, biased, σ_i	70	1.5e36	-26.55	274.66	158.55	8.6e-50
log $\mathcal{N}$, biased, $\bar{\sigma}_{17}$	52	4.9e26	-18.92	89.16	118.59	1.7e-09
log $\mathcal{N}$, biased, $\bar{\sigma}_9$	44	4.0e19	-2.26	64.86	114.09	0.0003

Table S7: Description of the three additional variance pools used for the modeling study, depending on the experimental conditions given in Table **S5**.

variance parameter	pooled experiments (state variable)
σ^4_{PKD}	8 (pPKD)
σ^5_{PKD}	10,11 (pPKD)
σ^6_{PKD}	13,14 (pPKD)

3.2 Selection of an error model

Analogous to model 1 we compared 12 different error models for the model 2 (Table **S6**). As before, AIC$_c$, BIC and Akaike weights agree on the choice of the best model, which is also with the additional experiments a normally distributed error model with standard deviations pooled over experiments and outputs. This results in 9 different standard deviations, six of which are the same as in Table **S3**, the other three ones are listed in Table **S7**.

4 Model 2: Modeling and model calibration

In the following we provide details on the negative feedback modeling approach and calibration to experimental data.

4.1 Modeling approach and normalization

Similar to model 1, we eliminated PKD and DLC1 by assuming mass conservation of respective total amounts

$$\text{PKD}_{\text{tot}} = \text{PKD} + \text{pPKD} \tag{16a}$$

$$\text{DLC1}_{\text{tot}}(1 + \alpha_5\theta_{12} - \alpha_6\theta_{13}) = \text{DLC1} + \text{pDLC1}. \tag{16b}$$

Table S8: Effect of different experimental treatments on the PKD phosphorylation rate $k(\mathrm{DLC1}, \theta)$ and on total DLC1 amounts

Treatment (u, α)	Effect on $k(\mathrm{DLC1}, \theta)$ or DLC1	Remark
–	$k = \begin{cases} \theta_0(1+\theta_6\mathrm{DLC1}) & \theta_6\mathrm{DLC1} \in (0,1] \\ 0 & \text{otherwise} \end{cases}$	unphosphorylated DLC1 increases the basal PKD phosphorylation rate
doxycycline	$\mathrm{DLC1} + \mathrm{pDLC1} = \mathrm{DLC1}_{\mathrm{tot}}(1+\theta_{12})$	doxycycline induces DLC1 expression and thus increases $\mathrm{DLC1}_{\mathrm{tot}}$
siDLC1	$\mathrm{DLC1} + \mathrm{pDLC1} = \mathrm{DLC1}_{\mathrm{tot}}(1-\theta_{13})$	siDLC1 reduces DLC1 expression
Rho ca	$k + \theta_9$	constitutively active Rho increases PKD phosphorylation
	$\theta_0(1+\theta_6\mathrm{DLC1}(1-\theta_{10}))$	feedback via Rock is negative
H1152	$\theta_0(1+\theta_6\mathrm{DLC1}(1+\theta_{11}))$	H1152 inhibits Rock activity and thus increases the overall PKD phosphorylation rate

Normalization of both state variables to total concentrations,

$$x_1 = \frac{\mathrm{pDLC1}}{\mathrm{DLC1}_{\mathrm{tot}}(1+\alpha_5\theta_{12}-\alpha_6\theta_{13})} \tag{17a}$$

$$x_2 = \frac{\mathrm{pPKD}}{\mathrm{PKD}_{\mathrm{tot}}} \tag{17b}$$

leads to

$$\begin{aligned}\dot{x}_1 = &(\theta_0(1+\tilde{\theta}_6(1+\alpha_5\theta_{12}-\alpha_6\theta_{13})(1-x_2)(1-\alpha_4\theta_{10})(1+\alpha_4\theta_{11})) \\ &+\theta_4 u_1+\theta_5 u_2+\alpha_3\theta_9)(1-\alpha_1\theta_7-\alpha_2\theta_8)(1-x_1)-\theta_1 x_1 \end{aligned} \tag{18a}$$

$$\dot{x}_2 = \tilde{\theta}_2(1-x_2)x_1 - \theta_3 x_2 \tag{18b}$$

where $\tilde{\theta}_2 = \theta_2\mathrm{DLC1}_{\mathrm{tot}}$ and $\tilde{\theta}_6 = \theta_6\mathrm{DLC1}_{\mathrm{tot}}$. Analogously to the first part, $\tilde{\theta}_2$ and $\tilde{\theta}_6$ will be called θ_2 and θ_6 in the following.

Changes in the DLC1 mediated PKD phosphorylation rate and the total DLC1 amount compared to model 1 are listed in Table **S8**. We note here that all experiments were conducted with doxycycline for model 1, while this is not the case for some of the additional experiments, such that we introduced an additional parameter to describe the effect of doxycycline addition on DLC1 total amounts.

4.2 Likelihood function

As before, the likelihood function for model 2 is given by

$$\mathcal{L}(\theta) = p(y|\theta) = \prod_{i=1}^{14}\prod_{j=1}^{2}\prod_{t_k}\prod_{l=1}^{4}\frac{1}{\sigma_{ij}\sqrt{2\pi}}\exp\left[-\frac{1}{2}\left(\frac{y_{ijl}(t_k)-z_{ij}(\theta,t_k)}{\sigma_{ij}}\right)^2\right] \tag{19}$$

with unknown parameter vector

$$\boldsymbol{\theta} = (\theta_0,\ldots,\theta_{13},\, \sigma^1_{\mathrm{PKD}},\ldots,\sigma^6_{\mathrm{PKD}},\sigma^1_{\mathrm{DLC1}},\ldots,\sigma^3_{\mathrm{DLC1}}) \in \mathbb{R}^{23}.$$

4.3 Optimization details

For optimization we used again `Matlab 2016b` (64 bit) and the toolboxes `SBPD` and `SBTOOLBOX2` and the internal `Matlab` solver `ode15i` for integration with options set to `options.abstol = 1e-10` and `options.reltol = 1e-10`. Optimization was performed with the gradient-based optimizer `fmincon`

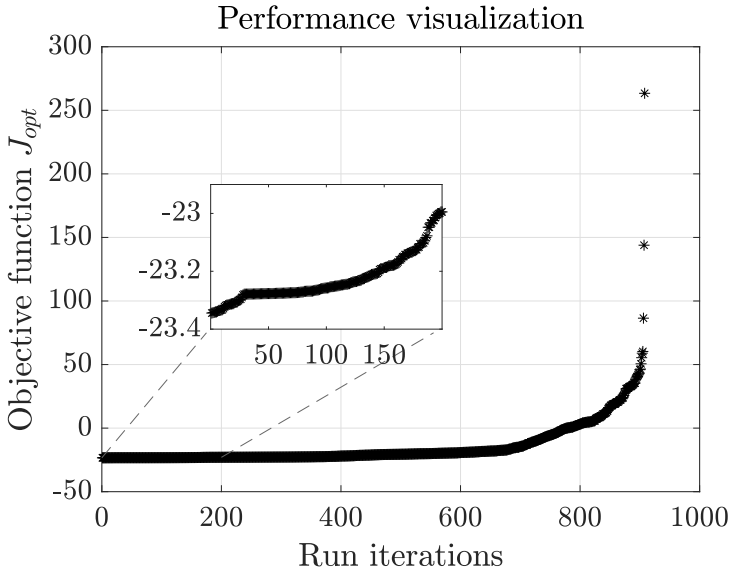

Fig S6: Sorted objective function values of converged parameter sets for model 2

with the interior point method and settings `OptionsFmincon.TolFun = 1e-6`, `OptionsFmincon.TolCon = 1e-6` and `OptionsFmincon.MaxFunEvals = 5000`.

As for model 1 we used a logarithmic scale for the parameters $\theta_0, \ldots, \theta_{13}$. The final boundaries of four orders of magnitude for these parameters were set after several optimization runs in order to avoid results on the boundaries. Following (18) the boundaries for θ_7, θ_8, θ_{10} and θ_{13}, the efficiencies of the two PKD inhibitors, Rho ca in the feedback and the silencing RNA for the total DLC1, were set to $[0, 1]$ without using a log-scale. Boundaries for the standard deviations σ_j^i were set around the empirical estimates, $\left[\frac{1}{2}\sigma_{\text{emp}},\, 2\sigma_{\text{emp}}\right]$. Optimization was performed with 1000 starting values from a latin hypercube sample. For all experiments the initial conditions $x_1(0)$ and $x_2(0)$ were assumed to be in a steady state and calculated accordingly. 908 starting points converged according to the step size criterion[2] for the parameter vector θ. As before, we evaluated the results according to the sorted J_{opt} values and took the first 150 values as a reasonable estimate for the global optimum, see Fig. **S6**.

A comparison of experimental data and model fits which are not shown in the main manuscript can be seen in Fig. **S7**. Shown are the time courses of pPKD and pDLC1 after stimulation with PDBu in the control case and with the PKD inhibitor kb-NB as well as the fold change in both variables induced by constitutively active Rho. The dynamic response of both variables is well captured in the control experiments, while the effect of the PKD inhibitor is underestimated, which is the opposite to the time series experiments after stimulation with nocodazole (Fig. 5) and thus a compromise model fit with respect to the efficiency of the inhibitor. The effect of Rho ca on both output variables is well captured. Compared to the model fit of model 1 trajectories show a larger variability.

Fig. **S8** shows the parameter scatterplots for model 2. Compared to that of model 1 parameters are more spread and less correlated. The parameters $\theta_1, \theta_7, \theta_8$ and θ_{12} are well identifiable. These are the PKD dephosphorylation rate, the effects of the two PKD inhibitors and the influence of doxycycline addition onto DLC1 total amounts. In contrast, the parameters θ_2 and θ_3, phosphorylation and dephosphorylation rates of DLC1, have a broad distribution. Some of the parameters also show correlations such as θ_4, θ_5 and θ_9, which are the influence of PDBu, nocodazole and RhoA on PKD phosphorylation.

Fig. **S9** shows that all standard deviations are well identifiable within the given bounds about the empirical values.

[2] ensuring that the change in the parameter vector is less than the specified step size tolerance and constraint violation is less than those specified in `options.ConstraintTolerance`

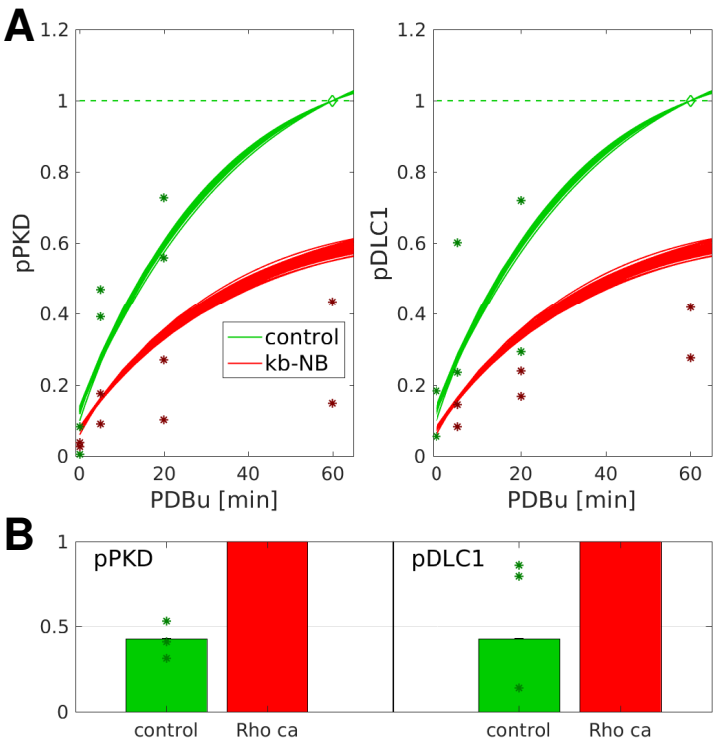

Fig S7: Fit for model 2. (A) Dots indicate re-normalized experimental data from Figs. 1 and **S1**, with normalization points indicated by diamonds, together with 150 estimated model trajectories.

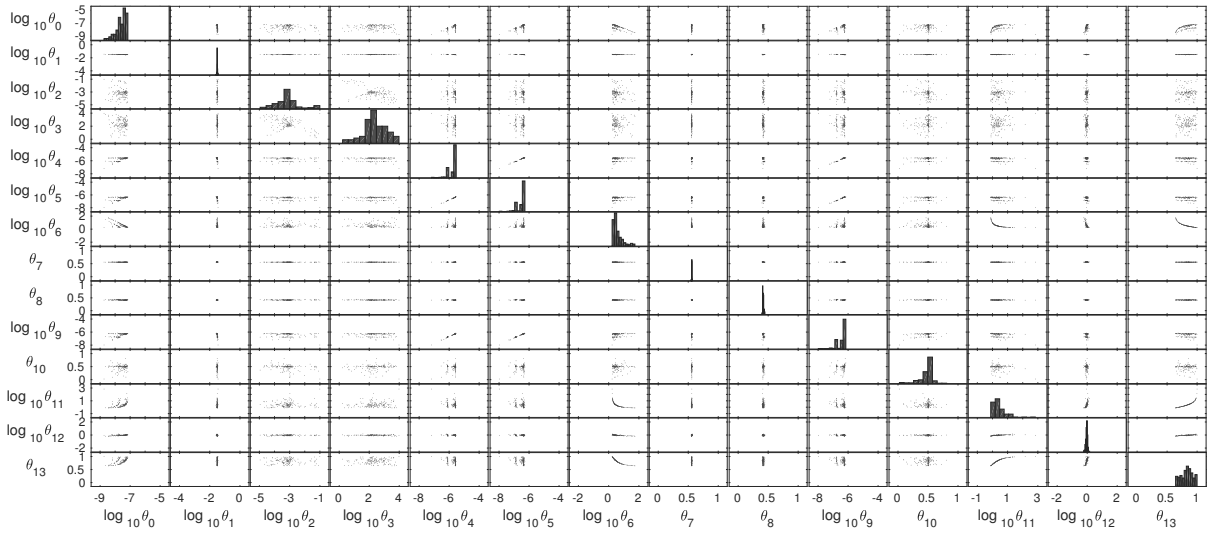

Fig S8: Scatterplot matrix for 929 parameter sets extracted from Fig. **S6** of model 2.

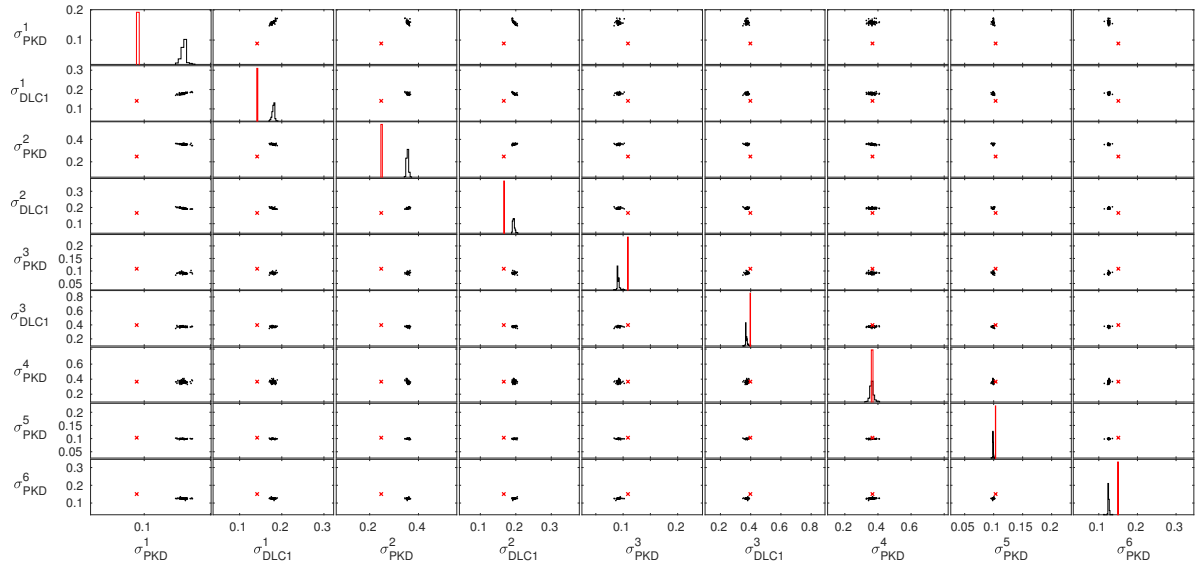

Fig S9: Scatterplot matrix of 150 estimated standard deviations σ_j^i (black) of model hypothesis 2 in comparison to unbiased empirical estimates σ_{emp} (red).

4.4 Model prediction

It is known that strong negative feedback can cause robustness of activity states to variations in total protein amounts for proteins in the feedback loop [5]. However, in our case it is unclear how to define the strength of the feedback loop. One possibility is to investigate the strengths of the individual links between the two components in our model. Thus, we simulated pDLC1 and pPKD fold changes implied by variations in PKD and DLC1 total amounts, respectively (top row in Fig. **S10**). pDLC1 increases in a perfect linear way with the PKD amount due to mass action kinetics for PKD mediated phosphorylation of DLC1. Similarly, pPKD is a linear function of the DLC1 amount, with an offset that corresponds to the basal and DLC1 independent PKD phosphorylation rate. Together, these results suggest that pPKD is highly influenced by DLC1 and vice versa. However, the conclusion that the overall feedback makes the system robust is not true in this case, as can be seen in Fig. **S10** (bottom row). Using mass action kinetics for a single molecule that is reversibly phosphorylated and not subject to feedback regulation, the phosphorylated protein amount is a linear function of the total amount. At the PKD level the system behaves exactly as such a decoupled system (left). This is different for DLC1 phosphorylation, were the effect of the negative feedback is visible in the deviation from the diagonal line (right). Thus, although we have strong influences between both output variables, this does not result in an overall strong effect of the negative feedback. An explanation for this paradigm is shown in Fig. **S10**. When pPKD and pDLC1 fractions are small, fold changes in pDLC1 implied by variations in PKD amounts might be large, but at the same time, the fold change in unphosphorylated DLC1, which feeds back to PKD, is so small that the effect of changes in PKD amounts are not propagated by the feedback.

5 Additional experiments

Fig. **S11** shows that DLC1 depletion by independent siRNAs reduces PKD activation in HEK293T cells and endogenous DLC1 localizes to focal adhesions in U20S cells.

References

[1] H. Akaike. Information theory and an extension of the maximum likelihood principle. pages 267–81, 1973.

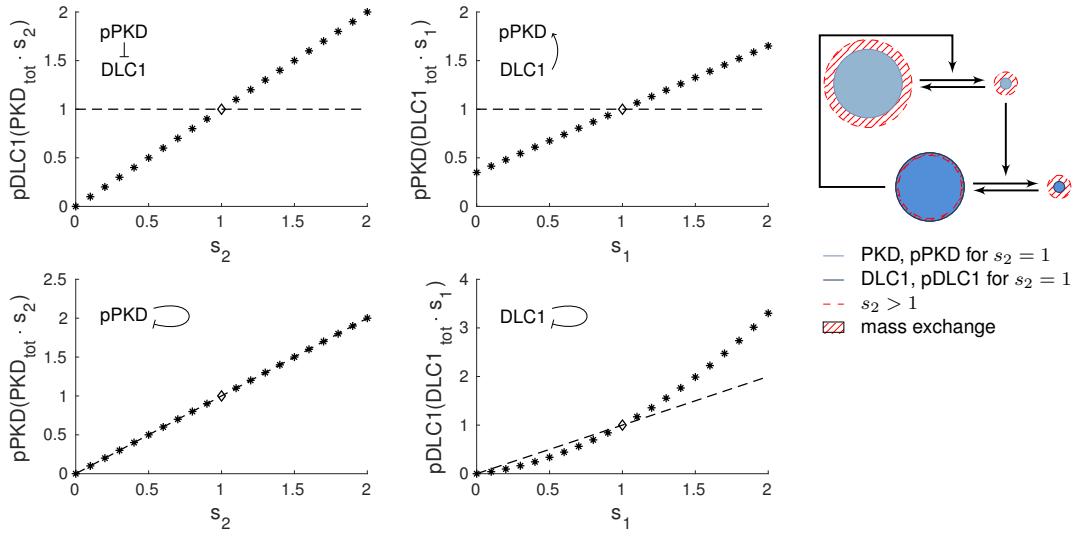

Fig S10: Interaction strengths between variables in the feedback loop. Normalization to nominal value denoted by diamonds. Top: Mutual influences between pPKD and pDLC1 are strong. Bottom: This does not result in a strong overall feedback and robustness of phosphorylated amounts against variations in respective total amounts. An explanation for this putative contradiction are small fractions of phosphorylated amounts.

[2] J.E. Cavanaugh. Unifying the derivations of the akaike and corrected akaike information criteria. *Stat Probabil Lett*, 31:201–8, 1997.

[3] A. Degasperi, M.R. Birtwistle, N. Volinsky, J. Rauch, W. Kolch, and B.N. Kholodenko. Evaluating strategies to normalize biological replicates of western blot data. *PLoS One*, 9(1):e87293, 2014.

[4] B. Efron. Bayesian inference and the parametric bootstrap. *The annals of applied statistics*, 6(4):1971, 2012.

[5] R. Fritsche-Guenther, F. Witzel, A. Sieber, R. Herr, N. Schmidt, S. Braun, T. Brummer, C. Sers, and N. Blüthgen. Strong negative feedback from Erk to Raf confers robustness to MAPK signalling. *Mol Syst Biol*, 7(489), 2011.

[6] R. Hooke and T.A. Jeeves. "direct search"solution of numerical and statistical problems. *Journal of the ACM (JACM)*, 8(2):212–229, 1961.

[7] R.E. Kass and A.E. Raftery. Bayes factors. *J Am Stat Assoc*, 90(430):773–95, 1995.

[8] C. Kreutz, M.M.B. Rodriguez, T. Maiwald, M. Seidl, H.E. Blum, L. Mohr, and J. Timmer. An error model for protein quantification. *Bioinformatics*, 23(20):2747–53, 2007.

[9] G.E. Schwarz. Estimating the dimension of a model. *Ann Stat*, 6(2):461–64, 1978.

[10] C. Thomaseth and R. Radde. Normalization of western blot data affects the statistics of estimators. *IFAC-PapersOnLine*, 49(26):56 – 62, 2016.

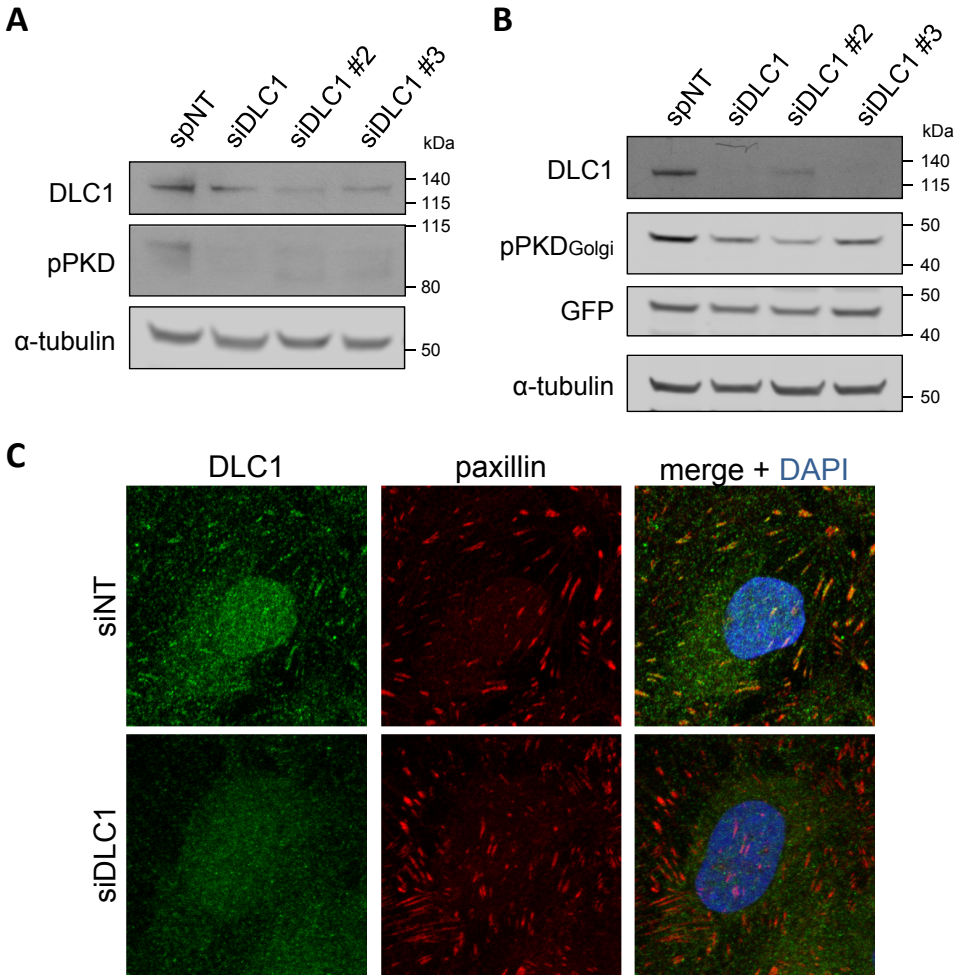

Fig S11: (A) HEK293T cells were transfected with the indicated siRNAs. After 3 days, cells were lysed and lysates were analyzed by immunoblotting. (B) Two days after transfection with the indicated siRNAs, HEK293T cells were transfected with the construct encoding the Golgi PKD activity reporter. The next day, cells were lysed and lysates analyzed by immunoblotting. (C) U2OS cells were transfected with the indicated siRNAs. After 3 days, cells were fixed and stained with DLC1 and paxillin specific antibodies, followed by fluorescently labeled secondary antibodies. Nuclei were counterstained with DAPI. The images shown are representative maximum intensity projections of several confocal sections.